for the manuscript

Modulatory ATP Binding Affinity in Intermediate States of E2P Dephosphorylation of Sarcoplasmic Reticulum Ca^{2+}-ATPase

by

Johannes D. Clausen, David B. McIntosh, David G. Woolley, and Jens Peter Andersen

TABLE S1

Affinities for MgF, vanadate, AlF, and BeF of SR and expressed wild type and mutants determined by inhibition of phosphorylation from $[\gamma\text{-}^{32}P]$ATP as described for Fig. S1. $K_{0.5}$ values are indicated relative (in %) to that of the expressed wild type obtained under the same conditions (for wild type the absolute $K_{0.5}$ value is shown bracketed). The S.E. is indicated with the number of experiments in parentheses.

	MgF	vanadate	AlF	BeF
Wild type	100 ± 3 (*n*=17) [0.55 mM]	100 ± 4 (*n*=21) [0.17 μM]	100 ± 5 (*n*=16) [10.1 μM]	100 ± 3 (*n*=20) [0.83 μM]
SR	138 ± 7 (*n*=2)	466 ± 73 (*n*=2)	208 ± 50 (*n*=2)	192 ± 19 (*n*=2)
R174A	92 ± 0 (*n*=2)	125 ± 11 (*n*=3)	78 ± 2 (*n*=2)	113 ± 17 (*n*=2)
R174E	103 ± 4 (*n*=2)	399 ± 6 (*n*=2)	111 ± 7 (*n*=2)	199 ± 14 (*n*=2)
I188A	178 ± 20 (*n*=2)	786 ± 47 (*n*=2)	396 ± 48 (*n*=2)	460 ± 45 (*n*=3)
I188F	86 ± 6 (*n*=2)	100 ± 0 (*n*=2)	103 ± 16 (*n*=2)	98 ± 2 (*n*=2)
K205A	61 ± 6 (*n*=2)	43 ± 4 (*n*=2)	38 ± 4 (*n*=2)	42 ± 2 (*n*=3)
E439A	167 ± 3 (*n*=2)	516 ± 18 (*n*=2)	262 ± 4 (*n*=2)	338 ± 76 (*n*=2)
F487L	84 ± 1 (*n*=2)	76 ± 6 (*n*=2)	82 ± 1 (*n*=2)	84 ± 12 (*n*=2)
F487S	ND[a]	ND[a]	ND[a]	ND[a]
R489L	59 ± 0 (*n*=2)	53 ± 5 (*n*=2)	56 ± 2 (*n*=2)	41 ± 0 (*n*=2)
K492L	160 ± 7 (*n*=2)	241 ± 6 (*n*=2)	269 ± 28 (*n*=2)	161 ± 10 (*n*=2)
R560L[b]	93 ± 14 (*n*=2)	155 ± 32 (*n*=2)	160 ± 3 (*n*=2)	98 ± 6 (*n*=2)
L562F	98 ± 22 (*n*=2)	135 ± 3 (*n*=3)	101 ± 11 (*n*=2)	98 ± 2 (*n*=2)
4Gi-46/47	71 ± 8 (*n*=2)	92 ± 12 (*n*=3)	69 ± 2 (*n*=2)	73 ± 9 (*n*=3)

[a]ND, not determined, because mutant F487S does not undergo phosphorylation under the present conditions for reaction with ATP (McIntosh *et al*. (1996) *J. Biol. Chem.* **271,** 25778-25789).
[b]Owing to the much reduced ability of mutant R560L to undergo phosphorylation from ATP (Clausen *et al*. (2003) *J. Biol. Chem.* **278,** 20245-20258), 50 μM ATP was used instead of 5 μM ATP for phosphorylation of this mutant. For comparison, phosphorylation of the wild type enzyme was carried out also with 50 μM ATP, and the results were indistinguishable from those obtained under the standard conditions with 5 μM ATP (not shown).
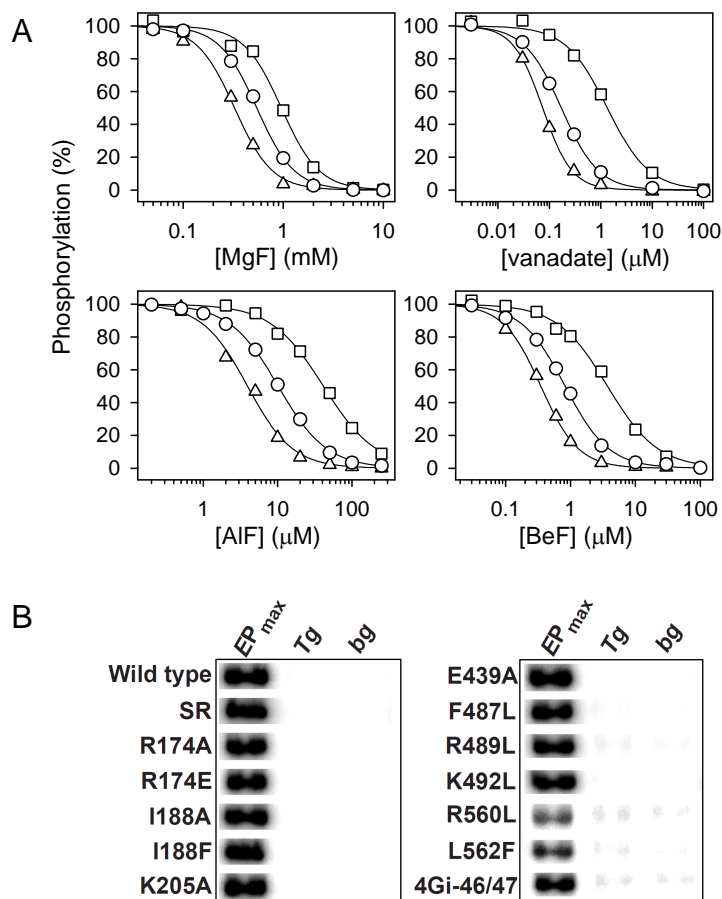
<u>Fig. S1.</u> **Sensitivity of wild-type Ca^{2+}-ATPase and mutants to MgF, vanadate, AlF, BeF, and Tg.** *A*, affinity for MgF, vanadate, AlF, and BeF determined by inhibition of phosphorylation from [γ-^{32}P]ATP. Data are shown for wild type (*circles*) and the two mutants, I188A (*squares*) and K205A (*triangles*), exhibiting the largest deviation from wild type (reduced and increased affinity, respectively). The affinity constants are listed in Table S1, along with those obtained in experiments carried out with SR and the remaining mutants. Microsomes were incubated for 30 min at 25 °C, followed by 10 min at 0 °C, in buffers containing 40 mM MOPS/Tris (pH 7.0), 80 mM KCl, 2 mM EGTA, and 5 mM NaF with varying concentrations of MgCl$_2$ ("MgF"), or 5 mM MgCl$_2$ with varying concentrations of orthovanadate ("vanadate"), or 2 mM NaF and 0.2 mM MgCl$_2$ with varying concentrations of AlCl$_3$ ("AlF"), or 0.2 mM MgCl$_2$ and 2 mM NaF with varying concentrations of BeSO$_4$ ("BeF"). The degree of inhibition was then determined by phosphorylation for 10 s at 0 °C with 5 μM [γ-^{32}P]ATP following addition of CaCl$_2$ to a final concentration of 2.5 mM (for MgF, vanadate, and AlF) or 2.1 mM (for BeF), giving a free Ca^{2+} concentration of 0.5 mM and 0.1 mM, respectively), and MgCl$_2$ to a final concentration of 5 mM. The level of phosphoenzyme obtained in the absence of inhibitor was taken as 100%. The *lines* show the best fits to the data of the Hill equation for inhibition, $EP = EP_{max} \cdot (1 - [L]^n / (K_{0.5}^n + [L]^n))$ (in which "L" is either MgF, vanadate, AlF, or BeF), giving the $K_{0.5}$ values listed in Table S1. *B*, autoradiographs of radioactive gels confirming the sensitivity of wild type and mutants to 1 μM Tg, as determined by the inhibition of phosphorylation from [γ-^{32}P]ATP. The lanes labeled "EP_{max}" (maximum phosphoenzyme) and "bg" (background) represent uninhibited enzyme. Wild type and mutant were incubated for 30 min at 25 °C in 25 mM MOPS/TMAH (pH 7.0), 80 mM

KCl, 2 mM EGTA, and either without ("EP_{max}", "bg") or with ("Tg") 1 µM Tg. The degree of inhibition was then determined at 0 °C by phosphorylation for 15 s following a 20-fold dilution of the microsomes into an ice-cold phosphorylation medium containing 40 mM MOPS/Tris (pH 7.0), 80 mM KCl, 5 mM $MgCl_2$, 5 µM [γ-^{32}P]ATP, and either 0.2 mM $CaCl_2$, giving a free Ca^{2+} concentration of 0.1 mM ("EP_{max}" and "Tg"), or 2 mM EGTA ("bg").
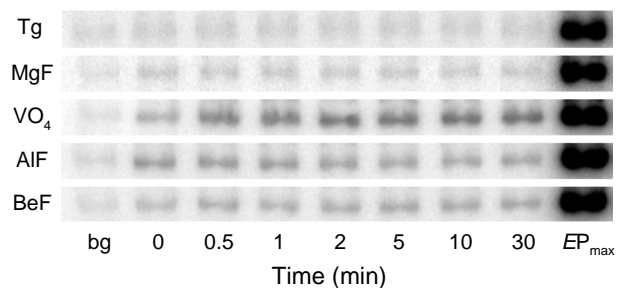
Fig. S2. **Stability of the $E2 \cdot Tg$, $E2 \cdot MgF$, $E2 \cdot$vanadate, $E2 \cdot AlF$, and $E2 \cdot BeF$ states of wild type Ca^{2+}-ATPase under photolabeling conditions.** Microsomes containing expressed wild type Ca^{2+}-ATPase were incubated with Tg, MgF, vanadate, AlF, or BeF as described under "Experimental Procedures", followed by 25-fold dilution of the microsomes into ice-cold medium containing 25 mM EPPS/TMAH (pH 8.5), 2 mM EDTA, and 17.4% (v/v) glycerol (*i.e.* same conditions as used in the photolabeling experiments) and incubation on ice for varying time intervals, as indicated on the *abscissa*. Next, the microsomes were phosphorylated with [γ-^{32}P]ATP for 15 s at 0 °C by supplementation with CaCl$_2$, MgCl$_2$, KCl, and [γ-^{32}P]ATP to final concentrations of 1.9 mM, 5.3 mM, 73 mM, and 5 μM, respectively, giving free Ca^{2+} and Mg^{2+} concentrations of 0.2 mM and 5.2 mM, respectively, and a MgATP concentration of 5 μM. The lanes labeled "bg" (background) and "EP_{max}" (maximum phosphoenzyme) represent uncomplexed enzyme. The background samples were supplemented with an excess amount of EGTA prior to phosphorylation, to chelate Ca^{2+} and thus prevent the reaction of the Ca^{2+}-ATPase with ATP. Only negligible dissociation of inhibitor occurred during 30 min incubation under photolabeling conditions, the reactivation during this period amounting to <5% for $E2 \cdot Tg$, $E2 \cdot MgF$, $E2 \cdot AlF$, and $E2 \cdot BeF$, and <10% for $E2 \cdot$vanadate. The 30 min is in fact much longer than the 60 s required to carry out the photolabeling (mixing of the enzyme into the labeling medium and subsequent transfer to the cuvette plus 35 s of irradiation).
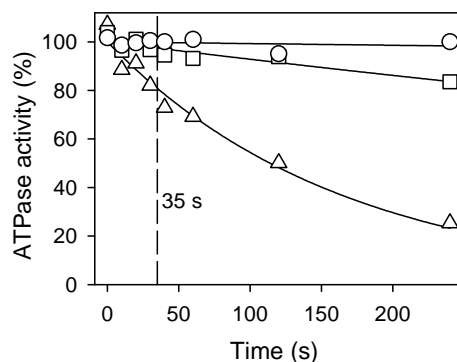
Fig. S3. **Stability of Ca^{2+}-ATPase activity during irradiation.** The short wavelength ultraviolet light from a xenon arc light source is potentially harmful to the protein. In our previous studies on TNP-8N$_3$-ATP photolabeling of the Ca^{2+}-ATPase the light beam was filtered by placing quartz cuvettes containing toluene in front of and behind the photolabeling cuvette, thereby ensuring that protein degradation was less than 3% (Seebregts and McIntosh (1989) *J. Biol. Chem.* **264,** 2043-2052). In the photolabeling setup used for the present study we replaced the toluene filter by a 295 nm wavelength cut-off glass filter. To test the efficiency of the glass filter the Ca^{2+}-ATPase activity was determined following irradiation for varying time intervals with (*squares*) or without (*triangles*) the glass filter mounted on the light source. The *circles* represent non-irradiated samples, treated otherwise exactly as the irradiated samples. It is seen that the glass filter was highly efficient in preventing loss of catalytic activity of the Ca^{2+}-ATPase. As with the previously applied toluene filter, less than 3% inactivation occurred with glass filter protection during the 35 s irradiation generally used in the photolabeling experiments (indicated by the *broken line*).
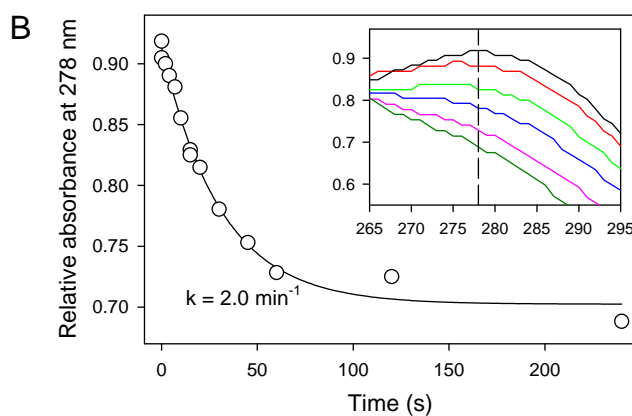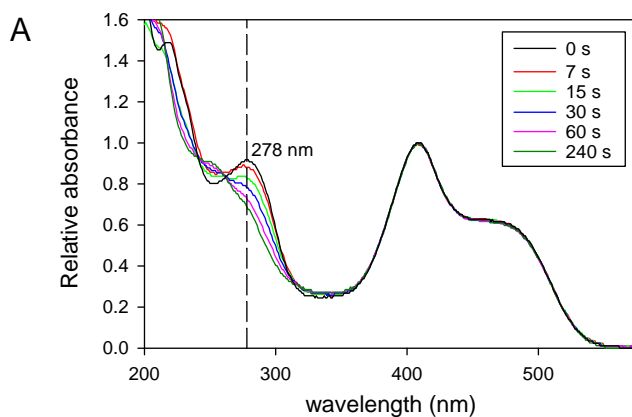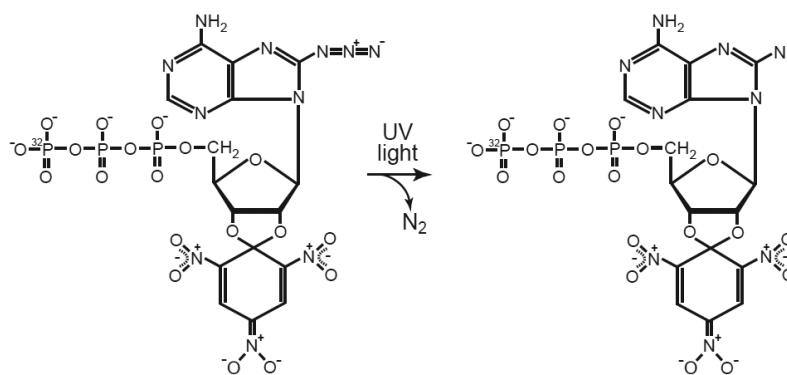
Fig. S4. **Time dependence of photolysis of the [γ-^{32}P]TNP-8N$_3$-ATP photolabel.** *A*, 100 μl of 10 μM [γ-^{32}P]TNP-8N$_3$-ATP in 10 mM potassium phosphate (pH 7.0) was irradiated for varying time intervals using the same irradiation setup as applied in the Ca^{2+}-ATPase photolabeling experiments, followed by recording of the absorbance spectrum. The absorbance maxima at 409 and 470 nm are contributed by the trinitrophenyl moiety of the nucleotide and that at 278 nm by the azido group, the absorbance of the latter decreasing upon irradiation owing to its degradation (cf. the reaction scheme above the panel). For comparison, the maximum absorbance at 409 nm was set to 1 for all time intervals, and spectra are shown for selected time irradiation times (cf. *inset*). *B*, graph showing the relative absorbance at 278 nm determined as described for panel *A* as a function of the time of irradiation. The *line* represents the best fit of a monoexponential decay function, $A = A_0 + A_{max} \cdot e^{-k \cdot t}$, to the data, giving a photolysis rate constant of 2.0 min^{-1}. The *inset* shows a close-up view of the absorbance around 278 nm from panel *A*.

7
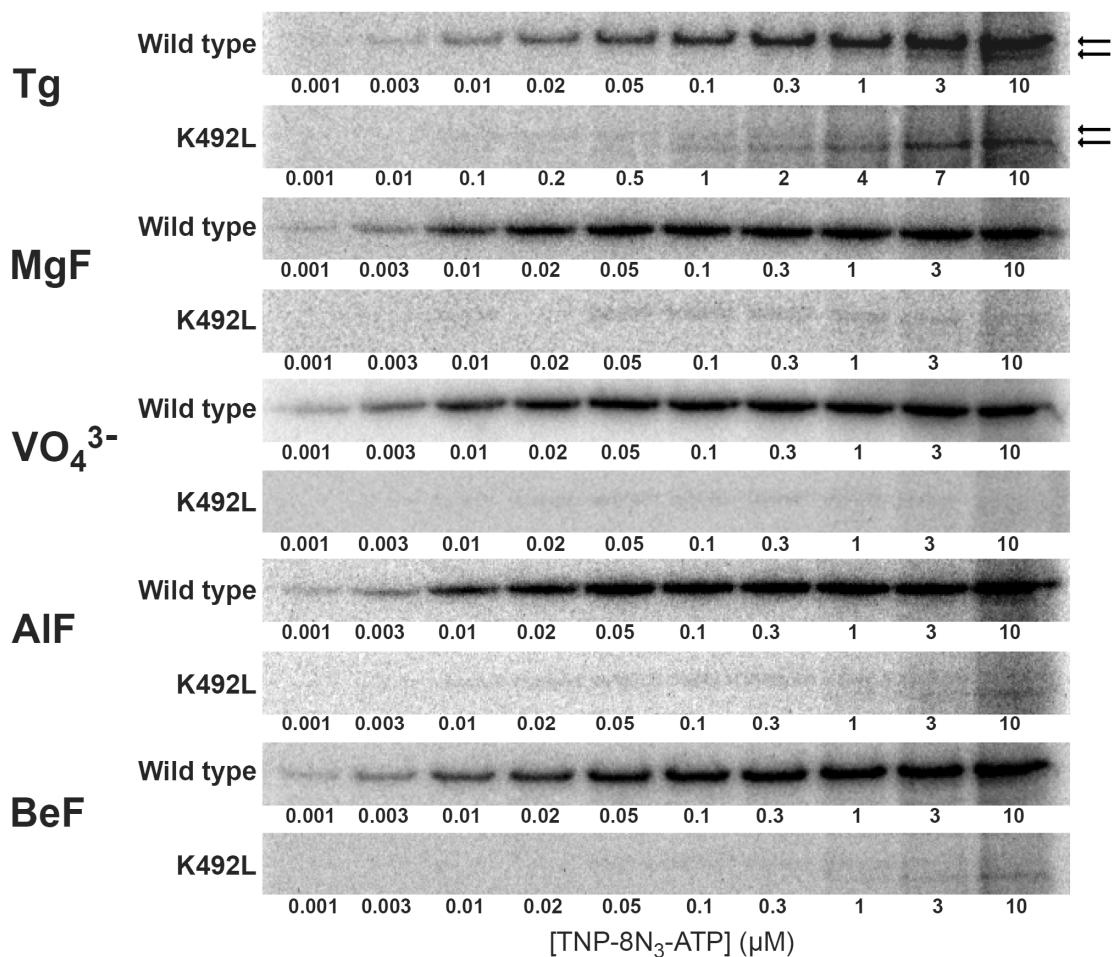
Fig. S5. **TNP-8N$_3$-ATP concentration dependence of photolabeling of wild type and mutant K492L complexed with Tg, MgF, vanadate, AlF, or BeF.** Expressed wild type or mutant K492L was incubated with Tg, MgF, vanadate, AlF, or BeF, and subjected to [γ-^{32}P]TNP-8N$_3$-ATP photolabeling. In general, at concentrations of TNP-8N$_3$-ATP below 1 μM the only photolabeled band visible on the gels was the band corresponding to the Ca^{2+}-ATPase. In some cases at higher TNP-8N$_3$-ATP concentration, bands corresponding to the photolabeling of other microsomal proteins began to appear on the autoradiograms, among these a band just below that of the Ca^{2+}-ATPase (the two bands are indicated by *arrows* in the two upper gels). The lower band is most easily visible in the gel corresponding to *E*2·Tg conditions, owing to the lower labeling levels of the Ca^{2+}-ATPase under these conditions compared with the vanadate and metal fluoride conditions as well as the fact that slightly higher concentrations of TNP-8N$_3$-ATP were applied in that particular experiment (cf. TNP-8N$_3$-ATP concentrations indicated below the gel). For mutant K492L, there was no discernible photolabeling of the Ca^{2+}-ATPase in any of the five complexed states, whereas the lower band appearing at higher TNP-8N$_3$-ATP concentration was visible to the same extent as for the wild type. The lack of ^{32}P-labeling of the K492L Ca^{2+}-ATPase protein implies that Lys^{492} is the photolabeled residue in the complexed states, as it is in the uncomplexed *E*1 state (McIntosh *et al*. (1992) *J. Biol. Chem.* **267,** 5301-5309).

8
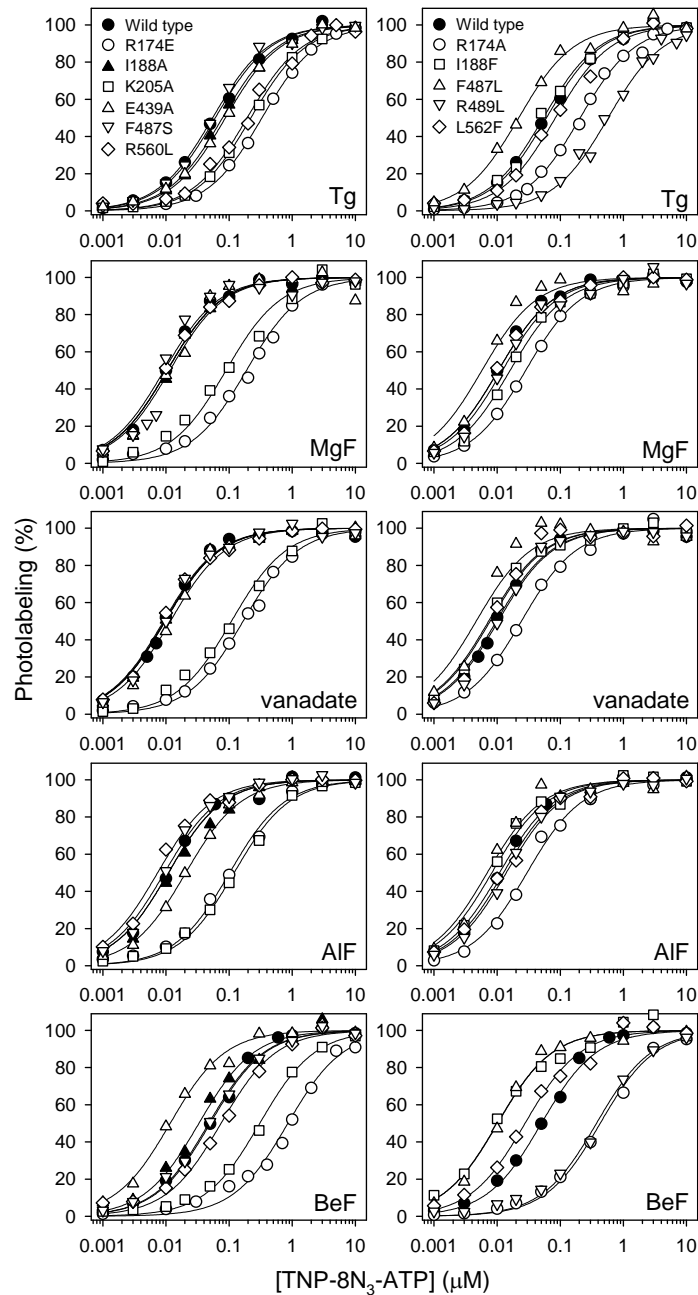
Fig. S6. **TNP-8N$_3$-ATP concentration dependences of photolabeling of Ca^{2+}-ATPase mutants stabilized in the intermediate states occurring during E2P dephosphorylation.** Expressed Ca^{2+}-ATPase was incubated with Tg, MgF, vanadate, AlF, or BeF as described under "Experimental Procedures", and subjected to TNP-8N$_3$-ATP photolabeling at the indicated concentrations of TNP-8N$_3$-ATP. In each case, the maximum level of specific labeling was defined as 100%. The affinity constants determined are listed in Table 1. Symbols for the five panels above each other are indicated in the top panel.

9
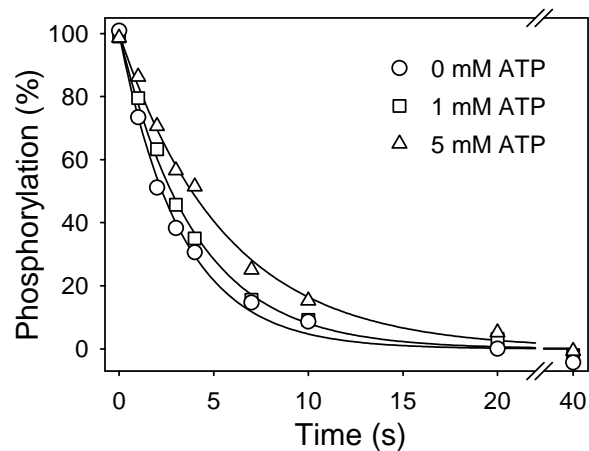
Fig. S7. **The rate of dephosphorylation of E_2P for mutant E439A at various ATP concentrations.** Examples of the data on which Fig. 6 is based, demonstrating the inhibition at high ATP concentration. The *lines* show the best fits of an exponential decay function, $EP = EP_{max} \cdot e^{-k \cdot t}$, giving the following rate constants: 0 mM ATP, $k = 18.4 \pm 0.6$ min^{-1} ($n = 6$); 1 mM ATP, $k = 15.2 \pm 1.1$ min^{-1} ($n = 2$); 5 mM ATP, $k = 10.9 \pm 0.5$ min^{-1} ($n = 3$).
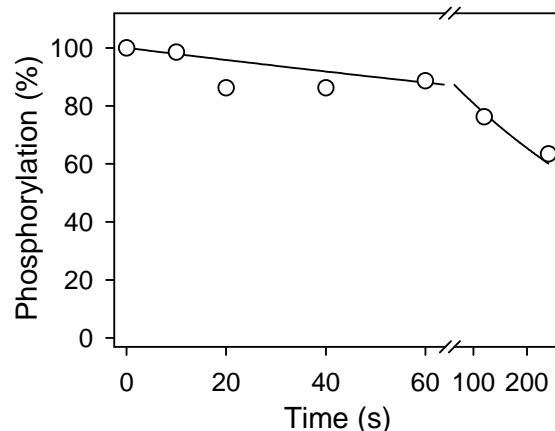
Fig. S8. **Stability of the Ca$_2$E2P state of mutant 4Gi-46/47 under photolabeling conditions.**
The Ca$_2$E2P state of mutant 4Gi-46/47 was formed as described under "Experimental Procedures". The accumulation of the Ca$_2$E2P state with mutant 4Gi-46/47 under these conditions has been verified previously (Daiho *et al*. (2007) *J. Biol. Chem.* **282,** 34429-34447; Clausen and Andersen (2010) *J. Biol. Chem.* **285,** 20780-20792). The stability of the Ca$_2$E2P phosphoenzyme was examined by 25-fold dilution of the phosphorylated and Ca^{2+}-saturated microsomes into ice-cold medium containing 25 mM EPPS/TMAH (pH 8.5), 2 mM EDTA, and 17.4% (v/v) glycerol (*i.e.* same conditions as used in the photolabeling experiments), followed by acid quench after varying time intervals as indicated on the *abscissa*. The duration of a photolabeling experiment, including mixing of the phosphorylated and Ca^{2+}-saturated microsomes into the photolabeling pre-mix and 35 s irradiation is less than 60 s, at which time ~90% phosphoenzyme still remains with mutant 4Gi-46/47. It can be assumed that the phosphoenzyme is indeed Ca^{2+}-saturated Ca$_2$E2P, because the Ca^{2+}-free E2P state of mutant 4Gi-46/47 is highly unstable, dephosphorylating at a rate equivalent to that of the wild type (Daiho *et al*. (2007) *J. Biol. Chem.* **282,** 34429-34447).